Synthesis, Characterization and *In Vitro* Anti-cancer Properties of Cationic Gemini Surfactants with Alkyl Chains in Human Breast Cancer

Anwar Shalan F. [1*], Samah Hussein Kadhim [1]

Abstract

Gemini surfactants have unique advantages in various industries such as detergents, cosmetics, paints, and pharmaceuticals due to their versatile hydrophilic-lipophilic balance. Three novel cationic surfactants, derived from alkyl alcohol and epichlorohydrin, featuring multi-alkyl multiple quaternary-ammonium salts, were synthesized with the order of C4 > C6 > C8 alkyl groups. The structure of the synthetic compounds was determined using FTIR and 1H-NMR analysis. The anti-cancer properties of the Gemini surfactants were determined with the MCF-7 breast cancer cell line, using the MTT cytotoxicity assay. We found an increase in alkyl groups (C4 > C6 > C8), indicating that larger alkyl groups contribute to improved surface qualities. The compounds showed improved surface qualities and reduced critical micelle concentration (CMC). In addition, The results showed the significant anti-cancer potential of compound B1 on the breast cancer cell line. In comparison to compounds B2 and B3, the highest inhibition was observed at concentrations from 25 to 400 µg/mL, demonstrating 26.8% to 4.3% and 32% to 4.7%, inhibition, respectively.

Keywords: Gemini surfactants, Hydrophilic-lipophilic, Cationic surfactants, Breast cancer, Anti-cancer

Significance | Anti-cancer activity of Gemini surfactants in human breast cancer cells

*Correspondence. Anwar Shalan F., Department of Chemistry, College of Science, University of Thi-Qar, Thi-Qar,64001, Iraq.
Email: anwarshalan112233@gmail.com

Editor Fouad Saleh Resq Al-Suede And accepted by the Editorial Board Jan 22, 2024 (received for review Dec 21, 2023)

1. Introduction

"Gemini surfactants" denotes a distinct class of cationic surfactants known as dimeric quaternary ammonium compounds. Comprising two monomeric moieties connected by a flexible or rigid spacer, each possesses a hydrophilic head group (a positively charged nitrogen atom) and a hydrophobic tail (a long alkyl chain) (A.R. Ahmady et al., 2022; B. Brycki et al., 2021). Gemini surfactants exhibit superior surface, interfacial, and biological characteristics compared to conventional monomeric counterparts (L. Lin et al., 2021; V. Kumar et al., 2020). The Critical Micelle Concentration (CMC) of Gemini surfactants is significantly lower than that of monomeric surfactants (V. Kumar et al., 2020). A lower CMC allows even a smaller amount of Gemini surfactant to achieve the desired effect (İ. Sarıkaya et al., 2021). The alkyl chains of Gemini surfactants reduce the CMC (Y. Liang et al., 2019; B. Brycki et al., 2019; J. Hao et al., 2019), while heteroatoms or a significant number of bonds in the spacer increase it (B. Brycki et al., 2019; E. Forsyth et al. 2020; H. Lal et al., 2022). Conversely, the spacer's length, flexibility, and the types of integrated groups can decrease or increase the CMC (C.S. Buettner et al., 2022).

Gemini surfactants find application in various fields, including biocides (H. Zhu et al., 2021), corrosion inhibitors (R. Aslam et al., 2019; M. Mobin et al., 2019), detergents (İ. Sarıkaya et al., 2021),

Author Affiliation.
[1] Department of Chemistry, College of Science, University of Thi-Qar, Thi-Qar,64001, Iraq.

Please cite this article.
Anwar Shalan F., Samah Hussein Kadhim, (2024). Synthesis, Characterization and In Vitro Anti-cancer Properties of Cationic Gemini Surfactants with Alkyl Chains in Human Breast Cancer, Journal of Angiotherapy, 8(1), 1-10, 9443

The alkyl chains of Gemini surfactants reduce the CMC (Y. Liang et al., 2019; B. Brycki et al., 2019; J. Hao et al., 2019), while heteroatoms or a significant number of bonds in the spacer increase it (B. Brycki et al., 2019; E. Forsyth et al. 2020; H. Lal et al., 2022). Conversely, the spacer's length, flexibility, and the types of integrated groups can decrease or increase the CMC (C.S. Buettner et al., 2022).

Gemini surfactants find application in various fields, including biocides (H. Zhu et al., 2021), corrosion inhibitors (R. Aslam et al., 2019; M. Mobin et al., 2019), detergents (İ. Sarıkaya et al., 2021), emulsifiers (D. Han et al., 2022), gene delivery agents (Z. Lu et al., 2023), micellar catalysis (A. Bhattarai et al., 2022; A.Z. Naqvi et al., 2021), and more. Their uses span the home, healthcare, pharmacy, and petrochemical industries (J. Feng et al., 2021; M. Akram et al., 2023; E.M.P. Gómez et al., 2022). However, their increased usage raises concerns about their potential environmental impact, as Gemini surfactants exhibit low biodegradability. Although compounds that do biodegrade can be digested by bacteria in the environment [3], dimeric surfactants threaten aquatic life, albeit less than their monomeric counterparts (R.A. Júnior et al., 2023). Altering the chemical makeup by adding ester links or substituting hydrophilic components can mitigate their aquatic toxicity and enhance biodegradability (D. Han et al., 2022; R.A. Júnior et al., 2023).

In the current study, three cationic Gemini surfactants with C4, C6, or C8 alkyl chains, oxygen as a spacer, and a hydroxyethyl group linked to the positively charged nitrogen atoms were investigated for self-aggregation, biodegradability, and cytotoxicity.

2. Material and Methods

Chemical and Equipment

The Sigma-Aldrich Company provided the following materials and equipment: epichlorohydrin (98 percent purity), isatin (98 percent purity), butanol (98 percent purity), hexanol (98 percent purity), octanol (98 percent purity), 1,6-dibromo hexane (98 percent purity), ethyl acetate (99 percent purity), and ethanol (99.8 percent purity). The chemical shifts recorded in the NMR spectra of the produced Gemini surfactants were internally referred to as TMS [0 ppm], and the spectra were captured in DMSO. On a Thermo Electron Corporation Nicolet 380 FT-IR spectrophotometer, Fourier transform infrared (FT-IR) Spectroscopy was used to establish the structural features of these novel Gemini surfactants. Aluminum sheets were subjected to TLC under a homogenous silica gel sorbent layer with a 90 to 120 m thickness and a sorbent size of 5-17 (m). The electrical conductivity of the surfactant solution and a WTW Inolab cond 740 conductivity meter were used to calculate the CMC values (Germany).

Synthesis of Alkyl Glycidyl Ethers (I) (Scheme 1)

In the reaction vessel, alcohol (0.1 mol) was heated to 400C. TBAB (0.2g, 0.00063 mol), sodium hydroxide (6g, 0.15mol), and (25ml) hexane were added, and the mixture was agitated for 30 minutes at the same temperature. The temperature was between 38°C and 400°C, while epichlorohydrin (18.5g, 0.2 mol) was added drop by drop over 30 minutes. After adding the epichlorohydrin, the mixture was rapidly agitated for 2 to 6 hours. The organic layer was separated after cooling the reaction mixture. Under reduced pressure, the solvent was removed from the organic layer, and the remaining material was vacuum-distilled to produce (I), a yellow precipitate with a yield of 0.78 g and a 78 percent purity (L. Lin et al., 2019; E.E. Badr et al., 2017).

Synthesis of 1-(3-butoxy-2-hydroxypropyl) indoline-2,3-dione (II) (Scheme 1)

Potassium carbonate was dissolved in 20 ml of ethanol, and Isatin (1.8g, 0.0125 mol) was added while agitating the solution. The solution was then agitated for 20 minutes at room temperature. The compound (1.3g, 0.01 mol) was added, and the reaction mixture's temperature was held at 800°C for 24 hours. The created precipitate was filtered, recrystallized from the ethanol, and then dried under vacuum to yield (II) as brown precipitate, yielding 0.71g, 71%, and 167°C M.P.

Synthesis of 1,1-(hexane-1,6-diyl)bis(1-(3-butoxy-2-hydroxypropyl)-2,3-dioxoindolin-1-ium)bromide B_1 (Scheme 1)

Compound II (2.7g, 0.01mol) was dissolved in ethanol when the solution became clear, 1,6-dibromohexan (0.75g, 0.005 mol) was added to the solution and reacted for 48h at 60°C. The reaction progress was controlled by TLC (eluent = 0.5:2.5:10: KNO_3: H_2O: CH_3CN). The produced precipitate was filtrated, recrystallized from ethanol, and then dried under vacuum to afford B_1 as brown precipitate, yielding 0.77g, 77%, M.P. 158°C. Compounds B_2 and B_3 were prepared in the same way.

In vitro anti-cancer activity

Preparation of cell culture

The human colorectal carcinoma (HCT 116) cell line was initially cultivated under optimal incubator conditions. Cells reaching 70–80% confluence were selected for cell plating. The old medium was aspirated from the flask, and the cells were washed 2–3 times with sterile phosphate-buffered saline (PBS) (pH 7.4). After washing, trypsin was evenly distributed onto the cell surfaces, and the cells were incubated at 37°C with 5% CO2 for 1 minute. The flasks were gently tapped to aid cell segregation, and the trypsin activity was halted by adding 5 ml of fresh media (10% FBS). Cells were then counted, diluted to a final concentration of 2.5 × 10^5 cells/ml, and inoculated into wells (100 µl cells/well). The plates containing the cells were finally incubated at 37°C with an internal atmosphere of 5% CO2.

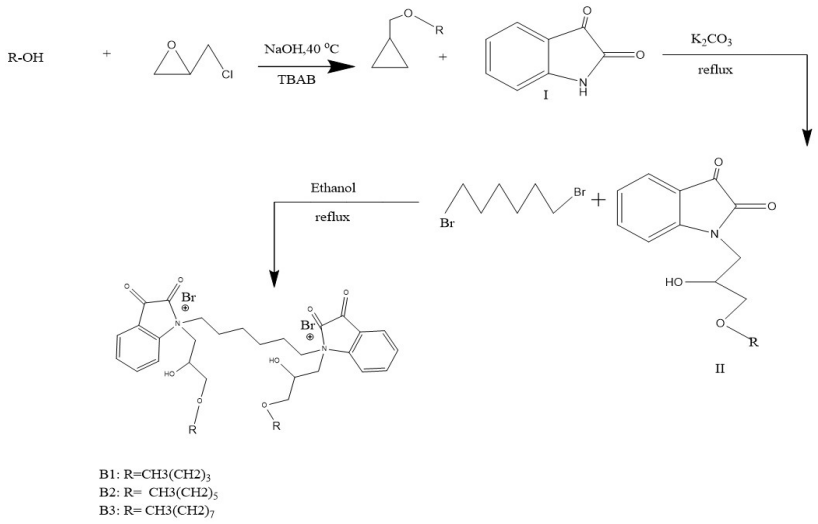

Scheme 1. Syntheses of Cationic Gemini Surfactants

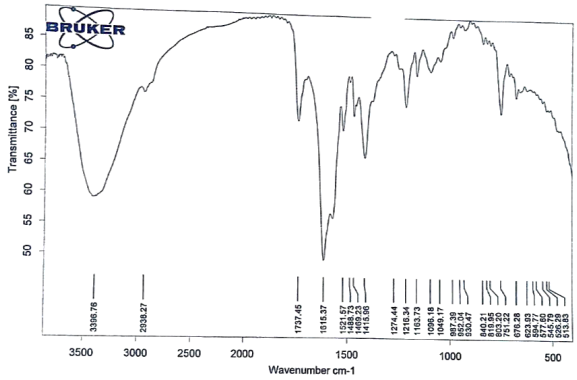

Figure 1. FT-IR spectra of cationic Gemini surfactants B_1.

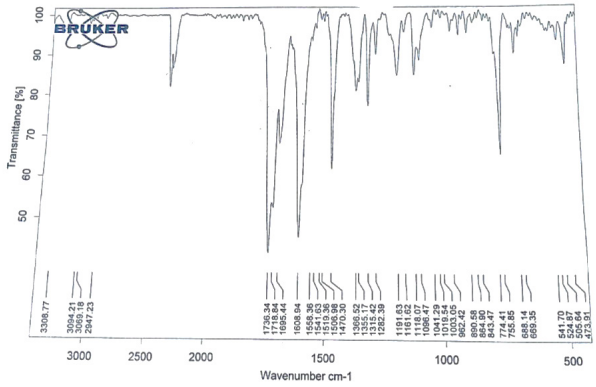

Figure 2. FT-IR spectra of cationic Gemini surfactants B_2.

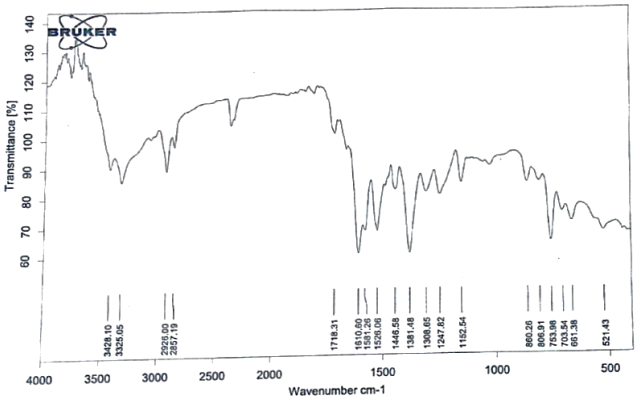

Figure 3. FT-IR spectra of cationic Gemini surfactants B_3.

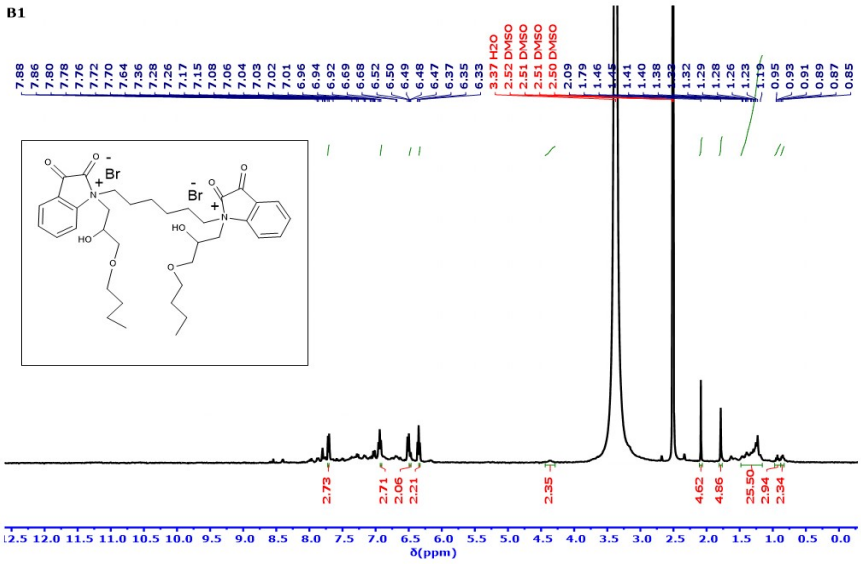

Figure 4. [1]H-NMR of cationic Gemini surfactants B_1.

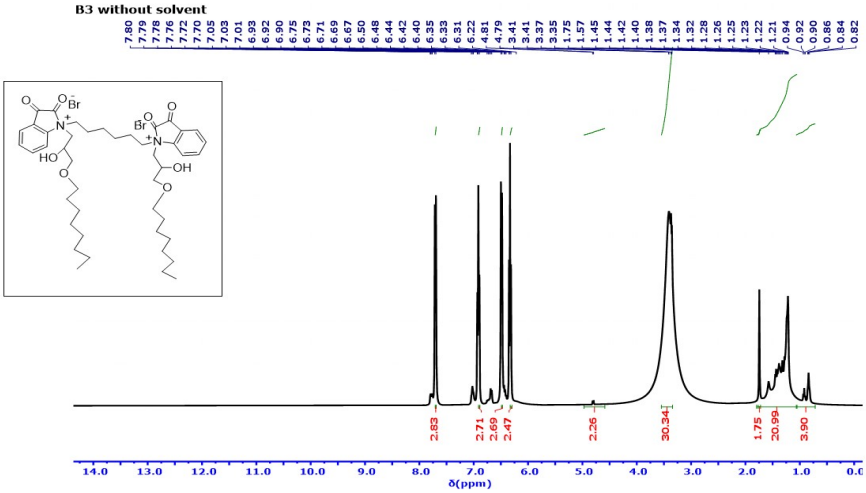

Figure 5. [1]H-NMR of cationic Gemini surfactants B_3.

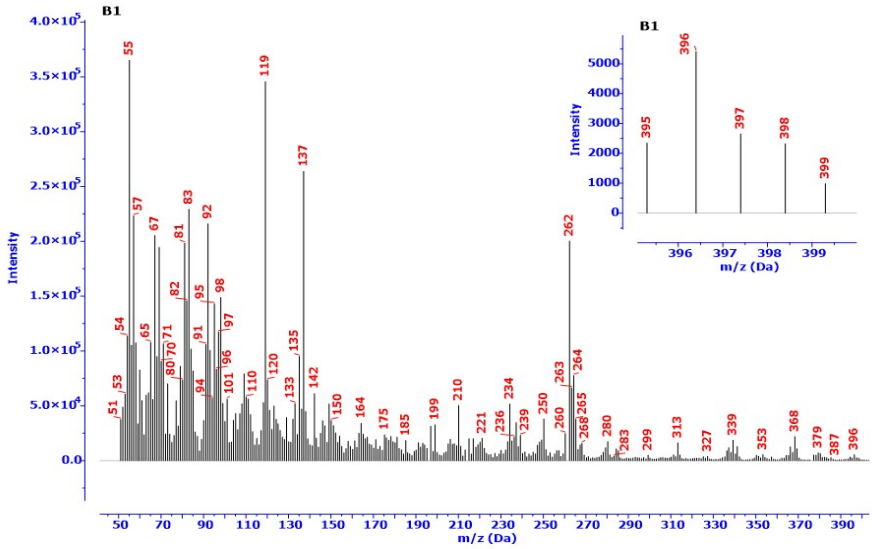

Figure 6. Mass spectra of cationic Gemini surfactants B_1.

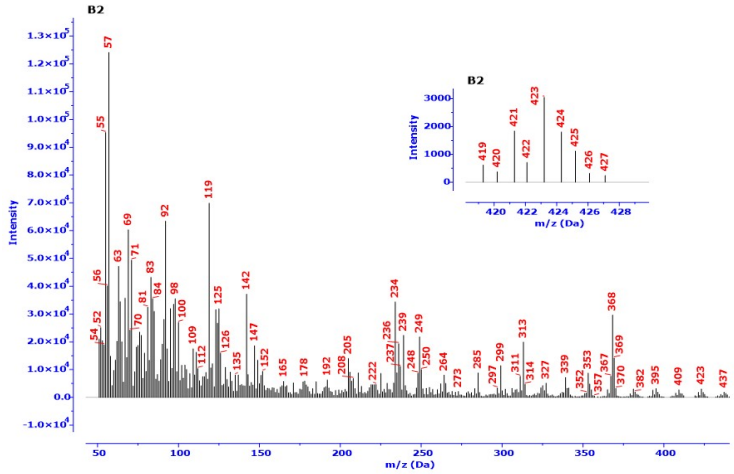

Figure 7. Mass spectra of cationic Gemini surfactants B_2.

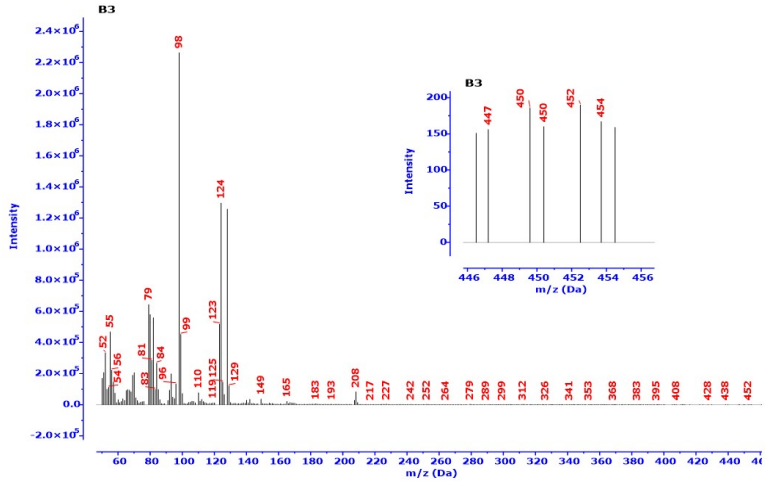

Figure 8. Mass spectra of cationic Gemini surfactants B_3.

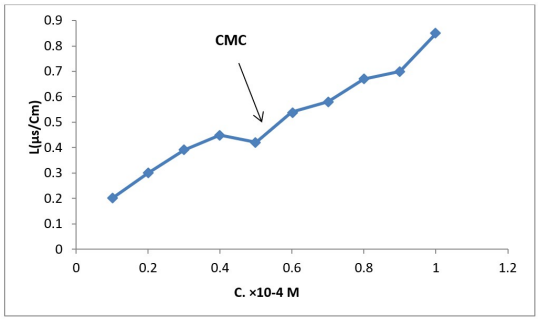

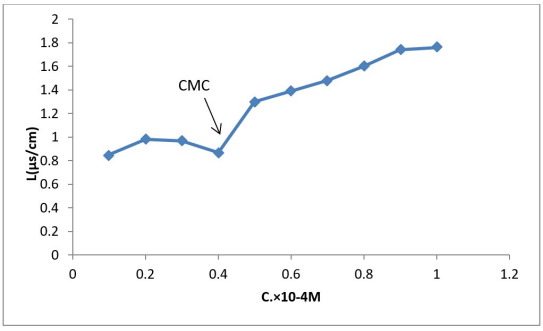

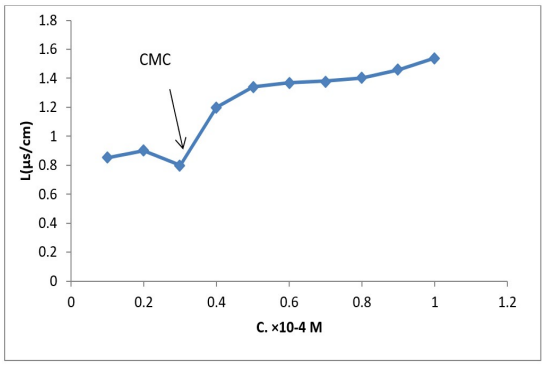

Figure 9. Critical micelles concentration of B_1 B_2 and B_3.

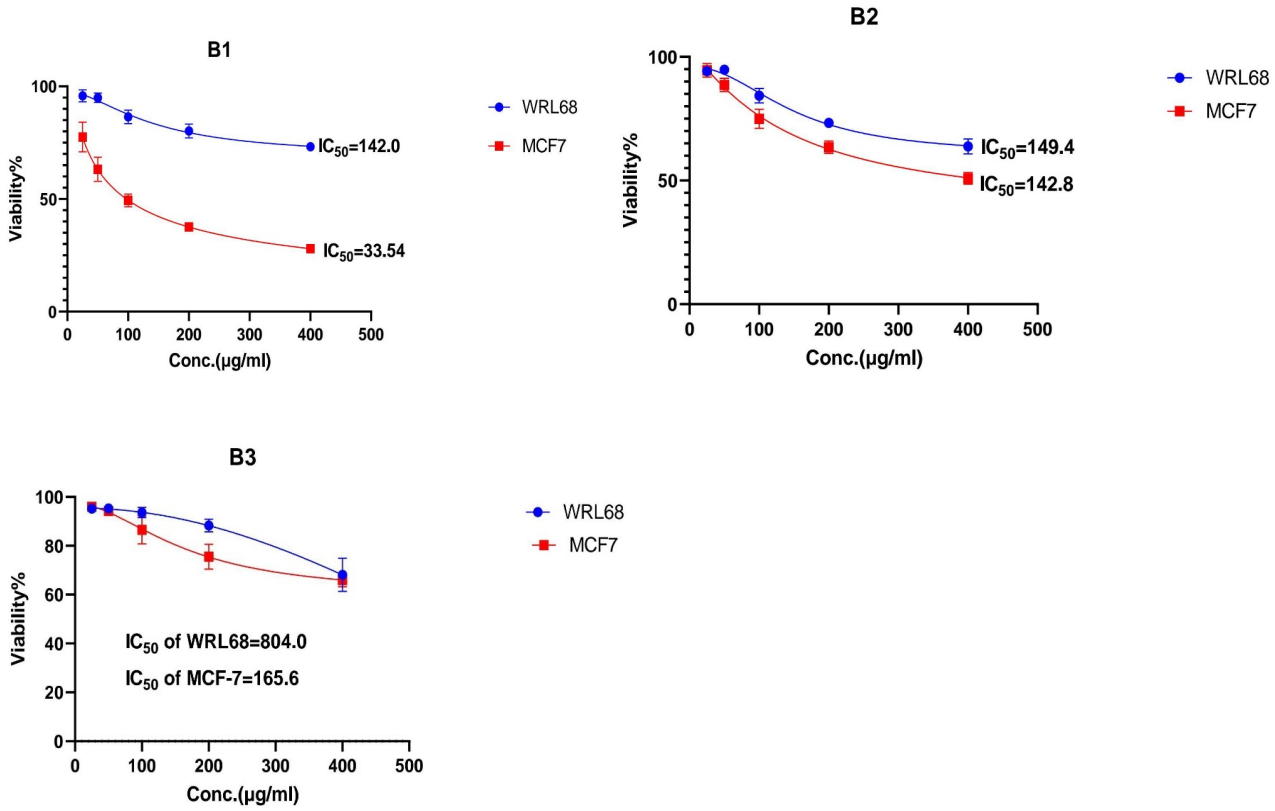

Figure 10. Effect of B_1, B_2 and B_3 compound on the cell line MCF-7 and WRL68 using the MTT test.

MTT assay

For the MTT assay, cancer cells (100 µl, 1.5 × 10^5 cells/ml) were inoculated into a 96-well microtiter plate. The plate was incubated overnight in a CO2 incubator to allow cell attachment. Subsequently, 100 µl of the test substance, diluted into desired concentrations from the stock with media, was added to each well containing the cells. The plates were then incubated at 37°C with an internal atmosphere of 5% CO2. After a 48-hour treatment period, 20 µl of MTT reagent was added to each well and incubated for 4 hours. Following this incubation, 50 µl of MTT lysis solution (DMSO) was added to each well. The plates were further incubated for 5 minutes in a CO2 incubator. Finally, the plates were read at 570 and 620 nm wavelengths using a monochromator-based multimode microplate reader (Tecan Infinite M1000 PRO). The data were recorded and analyzed to assess the effects of the test substance on cell viability and growth inhibition. The percentage of growth inhibition was calculated from the optical density (OD) obtained from the MTT assay.

3. Results and Discussion

FTIR Spectra

The FTIR test results for the compound B_1 are shown in Figure 1. The analysis showed that the synthetic product was the intended product because the vibration peak of -OH is 3396.76 cm^{-1}, the adsorption peak at 2938.27 cm^{-1} might be attributed to the asymmetric vibration of the CH_2 group, the peak of flexural vibration of C-H is 1469.23 cm^{-1}, the stretching band of C-O is 1216.3 cm^{-1}, the peak of C-N^+ is 1049.17 cm^{-1}, the peak of C=O is 1737 (A. Setyawati et al., 2017).

The FTIR spectrum of the chemical B_2 is shown in Figure 2. However, they were found for symmetric bending of CH_3 at 1315.42 cm^{-1}, CH_2 at 1470.30 cm^{-1}, and -$(CH_2)_n$- rock at 755.85 cm^{-1}. They were also found for C-O stretching at 1191.63 cm^{-1}, C-N^+ at 1041.29 cm^{-1}, C=O at 1736.34 cm^{-1}, and C=C at 1581.26 cm^{-1}. As can be seen, the vibration peak is 3308.77 cm^{-1} (A. Setyawati et al., 2017).

Figure 3 shows the characteristic bands for the alkyl part of compound B_3 at 2857.19 cm^{-1} for asymmetric stretching and 2926.00 cm^{-1} for symmetric stretching (CH), respectively. Asymmetric bending (CH_3) at 1308.65 cm^{-1}, symmetric bending (CH_2) at 1446.58 cm^{-1}, and symmetric bending $(CH_2)_n$-rock at 753.98 cm^{-1} were, nevertheless, found. Stretching bands for the elements C-O, C-N^+, C=O, and C=C measured 1247.82 cm^{-1}, 1152.54 cm^{-1}, 1718.31 cm^{-1}, and 1581.26 cm^{-1}, respectively; OH stretching measured 3428.10 cm^{-1}. The FTIR spectra of the synthesized molecule supported the predicted functional groups (A. Setyawati et al., 2017; S.H. Kadhim et al., 2022).

^{1}H-NMR Spectra

Figure 4 shows the outcomes of the generated B_1 compound's ^{1}H-NMR test.

^{1}H-NMR ($CDCl_3$): 0.87–0.93 (t, 6H, $(CH_3)_2$); 1.19–1.46 (m, 26H, $(CH_2)_{12}$–$(CH)_2$); 1.79 (t, 4H, (O- $CH_2)_2$); 2.09 (t, 4H, CH_2 CH_2); 4.36 (s, 2H, $(OH)_2$); 6.33–7.99 (m, 8H, Ar-H). It might be that the synthetic product was the target product by examining the relative areas of absorption peaks and peak positions of relative hydrogen atoms (S. Tang et al., 2022).

The ^{1}H-NMR spectra of B_3 Figure 5 demonstrated the occurrence of distinctive signals at 0.84-0.92(t, 4H, (O- $CH_2)_2$), 1.21-1.57 (m, 20H, $(CH_2)_{10}$), 1.75(s, 2H, $(CH)_2$), 3.5 (m, 30H, $(CH_2)_{12}$-($CH_3)_2$, 4.8(s, 2H, $(OH)_2$,6.3-7.8(m, 8H, Ar-H) (A. El Khetabi et al., 2020).

Mass Spectra

The mass spectrum of compounds B_1, B_2, and B_3 was analyzed. The molecular ion peak and isotope band appear in Figure 6, 7, 8.

Critical Micelle Concentration

The critical micelles concentration was evaluated for prepared surfactant at different concentrations (0.1-1) $\times 10^{-4}$ M. The electrical conductivity values were measured at 25°C, and the specific conductivity values were calculated by the equation (1). The critical micelles concentration (CMC) was calculated by plotting the conductivity with concentration, as shown in Figure 9. The CMC decreased with an increase in chain length and decreased with an increase in the polarity of compounds, with the order of compounds being B1 > B2 > B3 (A. Shadloo et al., 2022).

$$L = G \times A \quad (1)$$

Where, L =specific conductance, G=electrical conductivity, and A = cell constant.

Figure 9 illustrated the correlation between conductivity and concentration. With an increase in concentration, a greater number of amphiphilic molecules were introduced into the solution, resulting in a linear growth of conductivity until reaching the critical micelles concentration point (CMC). The substantial rise in conductivity was attributed to the liberation of additional free ions into the solution.

Anti-cancer properties of Cationic Gemini surfactant compounds

In this research, we utilized the MTT cytotoxicity assay to evaluate the toxicity of three water-soluble surfactant compounds on MCF-7 breast cancer cells (MSS Khan et al., 2016). Cell suspensions, ranging in concentration from 1×10^4 to 1×10^5 cells, were cultured in 96-well plates with a final volume of 200 micrometers of complete culture medium for each layer. After incubating at 37°C with 5 percent CO2 for 24 hours, we tested the cytotoxicity of Isatin compounds on breast cancer cells, specifically MCF-7.

For the B1 compound, we observed inhibition rates of 72.1%, 62.35%, 50.66%, 36.8%, and 22.5% at concentrations of 400, 200, 100, 50, and 25µg mL-1, respectively. Testing on the normal cell line WRL68 indicated inhibition rates ranging from 26.8% to 4.3%

at doses of 25 - 400µg mL-1 (Table 3). The IC50 calculation revealed a significant difference between the treatment of normal WRL68 (142.0µg mL-1) and MCF-7 cancer cells with the B1 compound (33.5 µg mL-1).

For the B2 compound, we observed inhibition rates of 49.12%, 36.58%, 25.0%, 11.3%, and 5.4% at 400, 200, 100, 50, and 25 µg mL-1 concentrations, respectively. Testing on the normal cell line WRL68 indicated inhibition rates ranging from 36.2% to 5.7% at 2 - 400 µg mL-1 concentrations. The IC50 calculation revealed substantial differences between the treatment of normal WRL68 (149.4 µg mL-1) and MCF-7 cancer cells with the B2 compound (142.8 µg mL-1).

For the B3 compound, inhibition rates of 34.1%, 24.5%, 13.4%, 5.8%, and 4.1% were observed at 400, 200, 100, 50, and 25 µg mL-1 concentrations, respectively. Testing on the normal cell line WRL68 indicated inhibition rates ranging from 32% to 4.7% at 25-400 µg mL-1 concentrations. The IC50 calculation revealed substantial differences between the treatment of normal WRL68 (804.0 µg mL-1) and MCF -7 cancer cells with the B3 compound (165.6 µg mL-1) (Figure 10)

4. Conclusion

In conclusion, three cationic Gemini surfactants with C4, C6, or C8 alkyl chains, oxygen as a spacer, and a hydroxyethyl group linked to the positively charged nitrogen atoms are investigated for self-aggregation, biodegradability, and cytotoxicity against the human breast cancer cells. Compound B1 showed strong potential against cancer, performing better than B2 and B3. It inhibited cancer cell growth by a notable amount, ranging from 22.5% to 72.1%. Taken together, these results provide useful information for designing and testing Gemini surfactants as possible treatments for cancer.

Author contribution

A.S.F. and S.H.K. conceptualized, performed the methodology, analsyzed the data and wrote the paper.

Acknowledgment

None declared.

Competing financial interests

The authors have no conflict of interest.

References

A. Bhattarai, M.A. Rub, M. Posa, B. Saha, A.M. Asiri, D. Kumar, (2022). Studies of ninhydrin and phenylalanine in cationic dimeric Gemini micellar system: Spectrophotometric and conductometric measurements, Colloids Surfaces A Physicochem. Eng. Asp. 655 (2022) 130334.

A. El Khetabi, R. Lahlali, L. Askarne, S. Ezrari, L. El Ghadaroui, A. Tahiri, J. Hrustić, S. Amiri, (2020). Efficacy assessment of pomegranate peel aqueous extract for brown rot (Monilinia spp.) disease control, Physiol. Mol. Plant Pathol. 110 (2020) 101482.

A. Setyawati, T.D. Wahyuningsih, B. Purwono, (2017). Synthesis and characterization of novel benzohydrazide as potential antibacterial agents from natural product vanillin and wintergreen oil, in: AIP Conf. Proc., AIP Publishing, 2017.

A. Shadloo, K. Peyvandi, A. Shojaeian, (2022). How the CMC adjust the liquid mixture density and viscosity of non-ionic surfactants at various temperatures?, J. Mol. Liq. 347 (2022) 117971.

A.R. Ahmady, P. Hosseinzadeh, A. Solouk, S. Akbari, A.M. Szulc, B.E. Brycki, (2022). Cationic gemini surfactant properties, its potential as a promising bioapplication candidate, and strategies for improving its biocompatibility: A review, Adv. Colloid Interface Sci. 299 (2022) 102581. https://doi.org/10.1016/j.cis.2021.102581.

A.Z. Naqvi, M. Panda, (2021). Mixed micellization: Improved physicochemical behavior of different amphiphiles in presence of gemini surfactants, J. Mol. Liq. 343 (2021) 116876.

B. Brycki, A. Szulc, (2021). Gemini surfactants as corrosion inhibitors. A review, J. Mol. Liq. 344 (2021) 117686. https://doi.org/10.1016/j.molliq.2021.117686.

B. Brycki, A. Szulc, H. Koenig, I. Kowalczyk, T. Pospieszny, S. Górka, (2019). Effect of the alkyl chain length on micelle formation for bis (N-alkyl-N, N-dimethylethylammonium) ether dibromides, Comptes Rendus Chim. 22 (2019) 386–392. https://doi.org/10.1016/j.crci.2019.04.002.

C.S. Buettner, A. Cognigni, C. Schroeder, K. Bica-Schröder, (2022). Surface-active ionic liquids: A review, J. Mol. Liq. 347 (2022) 118160.

D. Han, J. Mao, J. Zhao, H. Zhang, D. Wang, H. Cao, X. Yang, C. Lin, Y. Zhang, (2022). Dissipative particle dynamics simulation and experimental analysis of effects of Gemini surfactants with different spacer lengths on stability of emulsion systems, Colloids Surfaces A Physicochem. Eng. Asp. 655 (2022) 130205.

E. Forsyth, D.A. Paterson, E. Cruickshank, G.J. Strachan, E. Gorecka, R. Walker, J.M.D. Storey, C.T. Imrie, (2020). Liquid crystal dimers and the twist-bend nematic phase: On the role of spacers and terminal alkyl chains, J. Mol. Liq. 320 (2020) 114391. https://doi.org/10.1016/j.molliq.2020.114391.

E.E. Badr, (2017). Preparation, surface-active properties and antimicrobial activities of cationic surfactants based on morpholine and piperidine, Adv. Appl. Sci. Res. 8 (2017) 81–89.

E.M.P. Gómez, O.F. Silva, M. Der Ohannesian, M.N. Fernández, R.G. Oliveira, M.A. Fernández, (2022). Micelle-to-vesicle transition of lipoamino Gemini surfactant induced by metallic salts and its effects on antibacterial activity, J. Mol. Liq. 353 (2022) 118793.

H. Lal, M. Akram, (2022). Physico-chemical characterization of bovine serum albumin-cationic gemini surfactant interaction, J. Mol. Liq. 361 (2022) 119626.

H. Zhu, X. Li, X. Lu, J. Wang, Z. Hu, X. Ma, (2021). Efficiency of Gemini surfactant containing semi-rigid spacer as microbial corrosion inhibitor for carbon steel in simulated seawater, Bioelectrochemistry. 140 (2021) 107809.

İ. Sarıkaya, S. Bilgen, Y. Ünver, K. İnan Bektaş, H. Akbaş, (2021). Synthesis, characterization, antibacterial activity, and interfacial and micellar features of novel cationic gemini surfactants with different spacers, J. Surfactants Deterg. 24 (2021) 909–921. https://doi.org/10.1002/jsde.12532.

J. Feng, Z. Yan, J. Song, J. He, G. Zhao, H. Fan, (2021). Study on the structure-activity relationship between the molecular structure of sulfate gemini surfactant and surface activity, thermodynamic properties and foam properties, Chem. Eng. Sci. 245 (2021) 116857.

J. Hao, T. Qin, Y. Zhang, Y. Li, Y. Zhang, (2019). Synthesis, surface properties and antimicrobial performance of novel gemini pyridinium surfactants, Colloids Surfaces B Biointerfaces. 181 (2019) 814–821. https://doi.org/10.1016/j.colsurfb.2019.06.028.

L. Lin, H. Chu, K. Chen, S. Chen, (2019). Surface Properties of Glucose-Based Surfactants and Their Application in Textile Dyeing with Natural Dyes, J. Surfactants Deterg. 22 (2019) 73–83.

L. Lin, X. Li, J. Zhou, J. Zou, J. Lai, Z. Chen, J. Shen, H. Xu, (2021). Plasma-aided green and controllable synthesis of silver nanoparticles and their compounding with gemini surfactant, J. Taiwan Inst. Chem. Eng. 122 (2021) 311–319. https://doi.org/10.1016/j.jtice.2021.04.061.

M. Akram, M. Osama, H. Lal, M. Salim, M.A. Hashmi, K. Din, (2023). Biophysical investigation of the interaction between NSAID ibuprofen and cationic biodegradable Cm-E2O2-Cm gemini surfactants, J. Mol. Liq. 370 (2023) 120972.

M. Mobin, R. Aslam, J. Aslam, (2019). Synergistic effect of cationic gemini surfactants and butanol on the corrosion inhibition performance of mild steel in acid solution, Mater. Chem. Phys. 223 (2019) 623–633.

MSS Khan, AMSA Majid, MA Iqbal, ASA Majid. (2016). Designing the angiogenic inhibitor for brain tumor via disruption of VEGF and IL17A expression, European Journal of Pharmaceutical Sciences, 2016

R. Aslam, M. Mobin, J. Aslam, H. Lgaz, I.-M. Chung, (2019). Inhibitory effect of sodium carboxymethylcellulose and synergistic biodegradable gemini surfactants as effective inhibitors for MS corrosion in 1 M HCl, J. Mater. Res. Technol. 8 (2019) 4521–4533.

R.A. Júnior, J. de Faria Poloni, É.S.M. Pinto, M. Dorn, (2023). Interdisciplinary Overview of Lipopeptide and Protein-Containing Biosurfactants, Genes (Basel). 14 (2023).

S. Tang, X. Meng, F. Wang, Q. Lin, T. Feng, D. Hu, Y. Zhang, (2022). Four Propiconazole Stereoisomers: Stereoselective Bioactivity, Separation via Liquid Chromatography–Tandem Mass Spectrometry, and Dissipation in Banana Leaves, J. Agric. Food Chem. 70 (2022) 877–886.

S.H. Kadhim, (2012). Transition metal complexes with tridentate ligand 1E, 2E-ethanedial (2, 4-dinitro phenyl) hydrazone [5-(2-hydroxy phenyl)-1, 3, 4-oxadiazol-2-yl] hydrazone, J. Thi-Qar Sci. 3 (2012).

V. Kumar, N. Pal, A.K. Jangir, D.L. Manyala, D. Varade, A. Mandal, K. Kuperkar, (2020). Dynamic interfacial properties and tuning aqueous foamability stabilized by cationic surfactants in terms of their structural hydrophobicity, free drainage and bubble extent, Colloids Surfaces A Physicochem. Eng. Asp. 588 (2020) 124362. https://doi.org/10.1016/j.colsurfa.2019.124362.

Y. Liang, H. Li, M. Li, X. Mao, Y. Li, Z. Wang, L. Xue, X. Chen, X. Hao, (2019). Synthesis and physicochemical properties of ester-bonded gemini pyrrolidinium surfactants and a comparison with single-tailed amphiphiles, J. Mol. Liq. 280 (2019) 319–326. https://doi.org/10.1016/j.molliq.2019.02.018.

Z. Lu, G. Zongjie, Z. Qianyu, L. Xueyan, W. Kexin, C. Baoyan, T. Ran, R. Fang, H. Hui, C. Huali, (2023). Preparation and characterization of a gemini surfactant-based biomimetic complex for gene delivery, Eur. J. Pharm. Biopharm. 182 (2023) 92–102. https://doi.org/10.1016/j.ejpb.2022.12.002.